THERMAL BEHAVIOUR OF HIGH BURNUP PWR FUEL UNDER DIFFERENT FILL GAS CONDITIONS

T. TVERBERG
OECD Halden Reactor Project,
Halden, Norway

Abstract

During its more than 40 years of existence, a large number of experiments have been carried out at the Halden Reactor Project focusing on different aspects related to nuclear reactor fuel. During recent years, the fuels testing program has mainly been focusing on aspects related to high burnup, in particular in terms of fuel thermal performance and fission gas release, and often involving re-instrumentation of commercially irradiated fuel. The paper describes such an experiment where a PWR rod, previously irradiated in a commercial reactor to a burnup of ~50 MWd/kgUO_2, was re-instrumented with a fuel central oxide thermocouple and a cladding extensometer together with a high pressure gas flow line, allowing for different fill gas compositions and pressures to be applied. The paper focuses on the thermal behaviour of such LWR rods with emphasis on how different fill gas conditions influence the fuel temperatures and gap conductance. Rod growth rate was also monitored during the irradiation in the Halden reactor.

1. INTRODUCTION

Since most changes which occur in reactor fuel during irradiation are strongly temperature dependent, it is important that modelling codes provide good estimates of fuel temperatures. For this to be achieved, the codes obviously need to be validated through comparison with in-pile measurements. As target burnups in commercial reactors are being extended, more focus is being put on investigating the effects of increased burnup on in-pile performance and on implementing these in modelling codes. The Halden Reactor Project has over the years provided extensive data suitable for use in such code validation purposes; either through instrumentation fresh fuel but also, as has become increasingly important in recent years, re-instrumentation of commercially irradiated fuel.

Several phenomena need to be taken into account when analysing behaviour of high burnup fuel. The fuel-cladding gap closes during irradiation through fuel swelling and cladding creep down. Fission gas released from the fuel can reach the fuel-clad gap and decrease the gap conductance and thus increase fuel temperatures. Furthermore it has been shown, both through out-of-pile laser flash measurements and in-pile temperature measurements, that the thermal conductivity of the fuel degrades considerably with burnup [1, 2]. The instrumentation and areas subject to measurements with respect to thermal behaviour include, of course, above all fuel centre temperature measurements, but also pressure measurements for investigation of fission gas release and (for fresh fuel) fuel densification, fuel stack and clad elongation measurements to assess fuel densification and swelling rates. External gas lines providing the possibility to pressurize fuel rods at different pressure and gas composition provide means for investigating gap conductance and also gas flow measurements for investigation of hydraulic diameter and thus fuel-cladding gap in addition to assessing fission release.

This paper discusses an experiment performed in the Halden Boiling Water Reactor (HBWR) which provided several of the subjects mentioned above. A UO_2 rod, previously irradiated in a PWR reactor was re-instrumented with a fuel centre thermocouple, a cladding elongation

detector and external high- and low-pressure gas lines. During the irradiation in the HBWR, the rod was subject to several gas pressurization steps, using argon, up to as high as 300 bar overpressure while fuel temperature and clad elongation were monitored. The discussion of the data concentrates on the influence of gas composition and pressure on gap conductance and thus thermal behaviour in such a high burnup rod with a tight gap.

2. DESCRIPTION OF THE RIG AND TEST ROD

A schematic of the rig is shown in Fig. 1. The fuel segment used in this test was irradiated for 4 reactor cycles in a commercial PWR reactor. The discharge burnup was 52 MWd/kgUO_2. A simplified power history for the commercial irradiation is shown in Figure 2. During the final cycle of the commercial irradiation, the Linear Heat Rate (LHR) was ca. 20 kW/m.

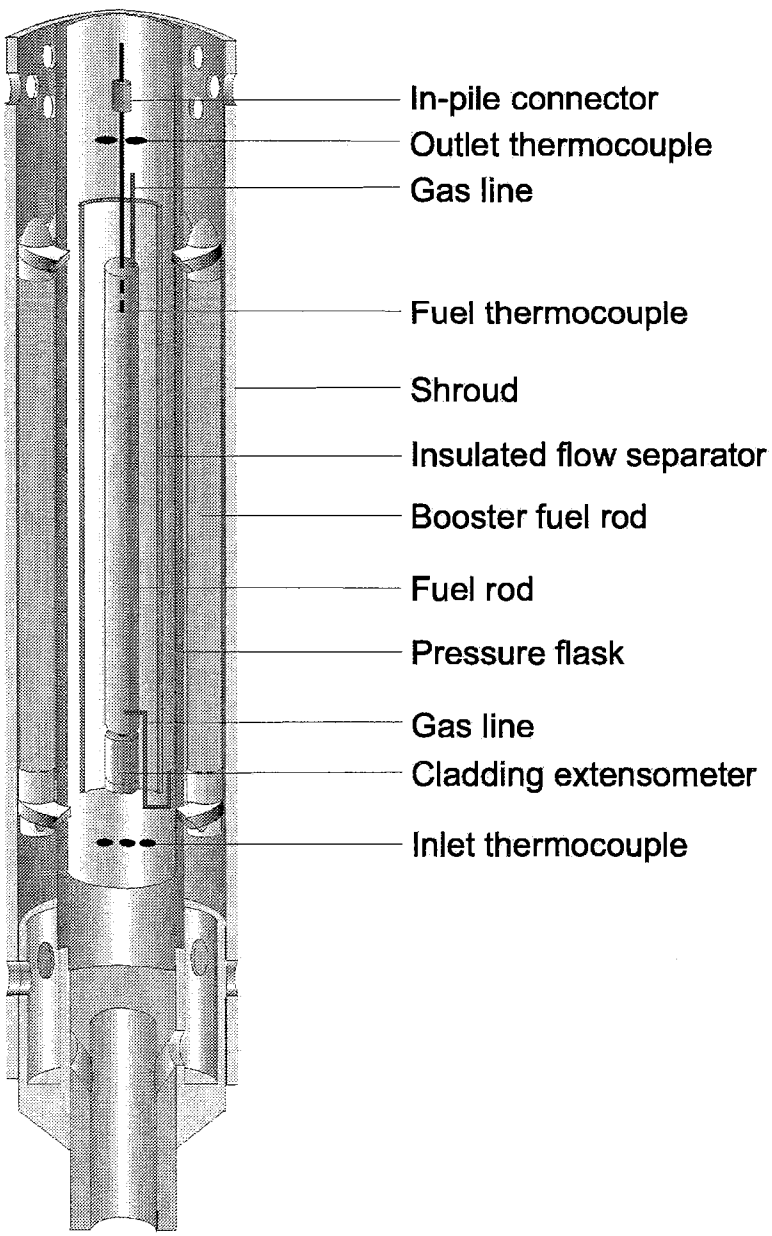

FIG. 1. Schematic of test rig.

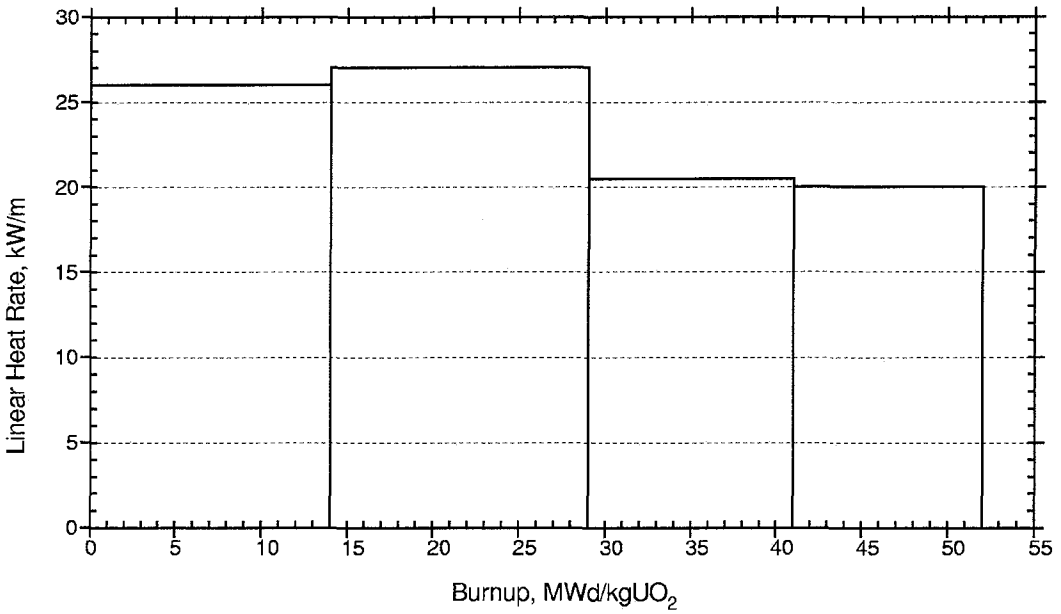

FIG. 2. Base irradiation history.

The testing in the HBWR was performed under simulated PWR conditions; i.e. ~160 bar coolant pressure at 310°C. The rod instrumentation consisted of:

- a fuel centre thermocouple (TF) in the upper end of the rod (ca. 40 mm drilled hole, 2.5 mm diam.)
- a clad extensometer in the lower end
- a high pressure system for pressurisation of the rod with argon
- a low pressure system to perform gas flow measurements for assessing hydraulic diameter. The low pressure system also allows for sweeping out fission gases to a spectrometry system.

In addition to the rod instrumentation, the rig was equipped with vanadium neutron detectors to monitor the axial flux distribution in the rig.

The test rig was situated inside a pressure flask which ensures the high pressure conditions of a PWR (~160 bar). To provide a fast neutron flux more representative of PWRs, the pressure flask was surrounded by 12 booster rods of PWR type with a high enrichment (13% U-235). The main characteristics of the fuel rod is summarized in Table I.

3. IN-PILE PERFORMANCE

3.1 Power history

The rod was irradiated for a total of 4400 full power hours (fph) and the burnup increase during the test was 4.1 MWd/kgUO_2. Fig. 3 shows the average linear heat rate and fuel temperature for the first 2300 fph. The heat rate varies slightly around 15 kW/m throughout this period.

During the irradiation, the pressure was changed in steps of ca. 50 bars by pressurizing with argon. In terms of gas thermal conductivity, Ar corresponds to a Xe/He gas mixture of about 70%/30%. The fuel temperature stays at ca. 700°C during this period. Indicated in the plot is also the peak fuel temperature, which is estimated through calculating the difference between the temperatures of a solid and hollow pellet, the difference being ca. 100°C.

TABLE 1. FUEL ROD FABRICATION DETAILS

Parameter	
Fuel Enriched Length (mm)	422
Fuel Weight (g)	273.5
Initial Density (% of T.D.)	96.1
Initial Enrichment (w/o U^{235})	3.8
Grain Size (□m)	8.5
Initial Fuel - o.d. (mm)	9.12
Fuel - i.d. - for TF (mm)	2.5
Thermocouple Penetration (mm)	~40
Clad Material/Heat Treatment	Zr-4 (partly recrystallised)
Initial Clad - o.d. (mm)	10.75
Initial Clad - i.d. (mm)	9.29
Initial diametral gap (□m)	170.
Fill Gas/Pressure Base Irr. (bar)	He/21.5
Instrumentation	TF1/EC1
Burnup (MWd/kgUO_2)	52.
Oxide layer (μm)	40–60

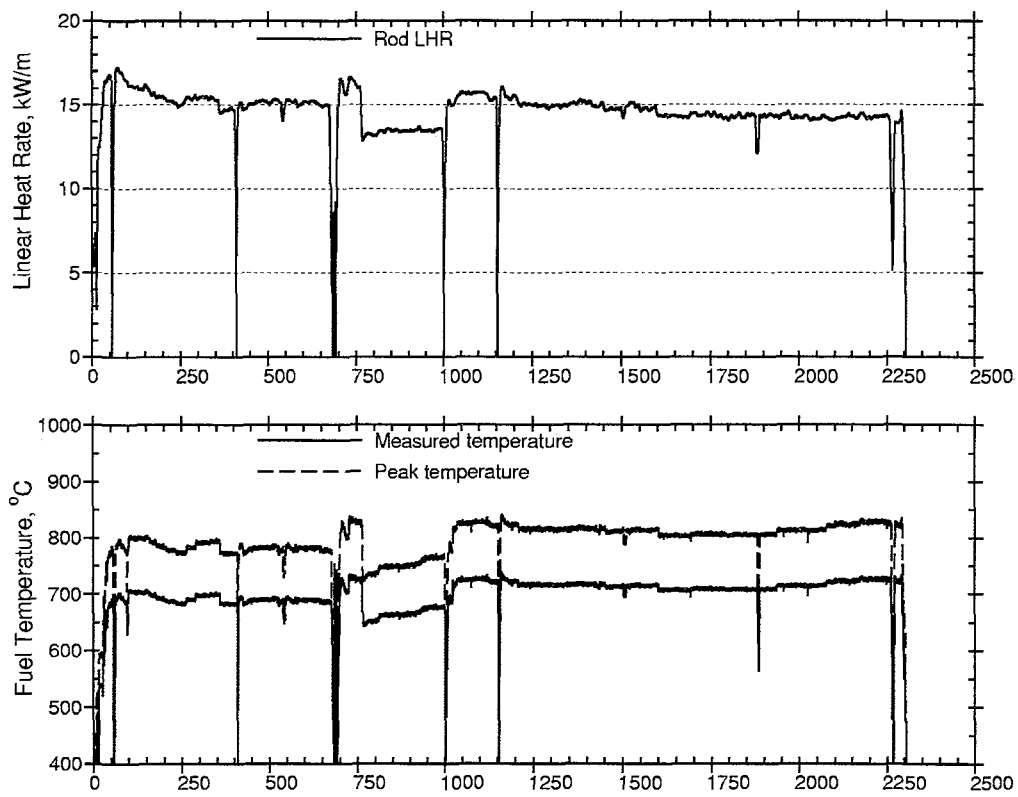

FIG. 3. Average linear heat rate and fuel temperature versus full power hours.

3.2 Clad elongation behaviour

Fig. 4 shows the measured clad elongation and average heat rate for the same period as Fig. 3. The clad elongation follows the rod power fluctuations, indicating that there is pellet-clad contact throughout the period. This can also be seen in Fig. 5, where measured elongation is plotted versus AHR for various power ramps. The dashed lines in the figure are estimated clad free thermal expansion curves. The measured elongation deviates from the clad free thermal expansion at powers 10–15 kW/m indicating that gap closure occurs at this power level.

Elastic deformations can be seen for each step in pressure. Fig. 6 shows a close-up of such a pressure step where the observed elastic deformation induced by the pressure increase is 28 μm. For the other pressurisations that were performed, the elastic deformation was in the same order.

A tendency of permanent increase in elongation in the same range as what could be expected from solid fission product fuel swelling can be seen (the dashed curve included in the plot indicates a swelling rate of 0.7% ΔV/V per 10 MWd/kgU). This is similar to what has been observed for other rods in the same burnup range [3], where clad elongation increase was found to be indicative of fuel swelling.

3.3 Fuel temperature response to pressurisation

Fig. 7 shows the temperature-power relation for two early power ramps. The first ramp shown is from before the first argon pressurization, i.e. helium at low pressure. The second ramp is after ca. 400 fph when the rod was pressurized to +100 bar Ar. The dashed lines in the plot are least square fits to the data. The influence of gas change on the temperature is small, but measurable. At a heat rate of 12 kW/m the observed temperature increase is ca. 20°C.

Fig. 8 shows the same ramps as Fig. 7 together with two additional ramps at rod overpressure +100 and +200 bar respectively. Between the two +100 bar ramps, the temperature increases further (again, ca. 20°C at 12 kW/m), whereas for the +200 bar ramp, the temperature-power relation remains unchanged from the previous +100 bar ramp. In the following sections, possible explanations for the observed temperature behaviour will be discussed.

4. DATA EVALUATION

4.1 Assumptions used in the model

For such high burnups as in the case of this rod, experience has shown that the radial distribution of burnup and porosity will be highly non-uniform. Also the radial power distribution will be very different from the case for fresh fuel. In the calculations used hereafter, the radial power, burnup and porosity have been assessed according to the TUBRNP model [4]. An example of calculated power and burnup distribution is shown in Fig. 9.

It has been shown, both from in-pile and laser flash measurements, that fuel thermal conductivity degrades significantly with burnup. In the calculations, this degradation has been taken into account using the following modified correlation for UO_2 conductivity [5]:

$$\lambda = \frac{1}{0.1148 + 0.0040 \cdot B + 2.475 \cdot 10^{-4} \cdot (1 - 0.00333 \cdot B) \cdot \delta + 0.0132 \cdot e^{0.00188 \cdot T}}$$

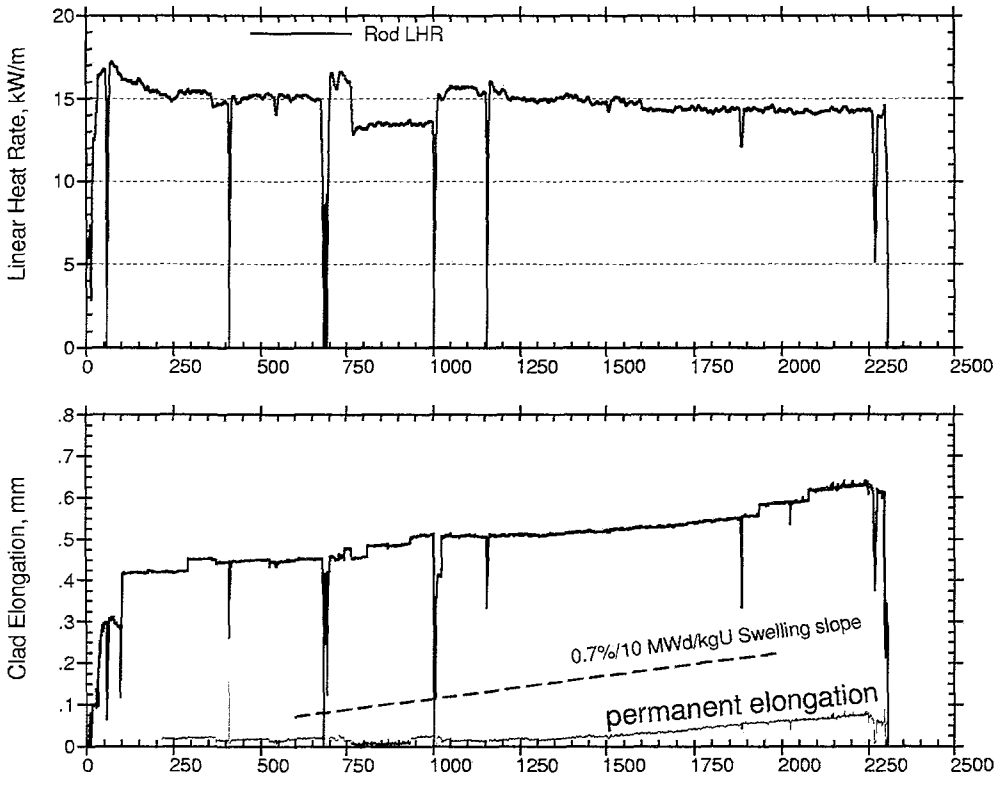

FIG. 4. Clad elongation history.

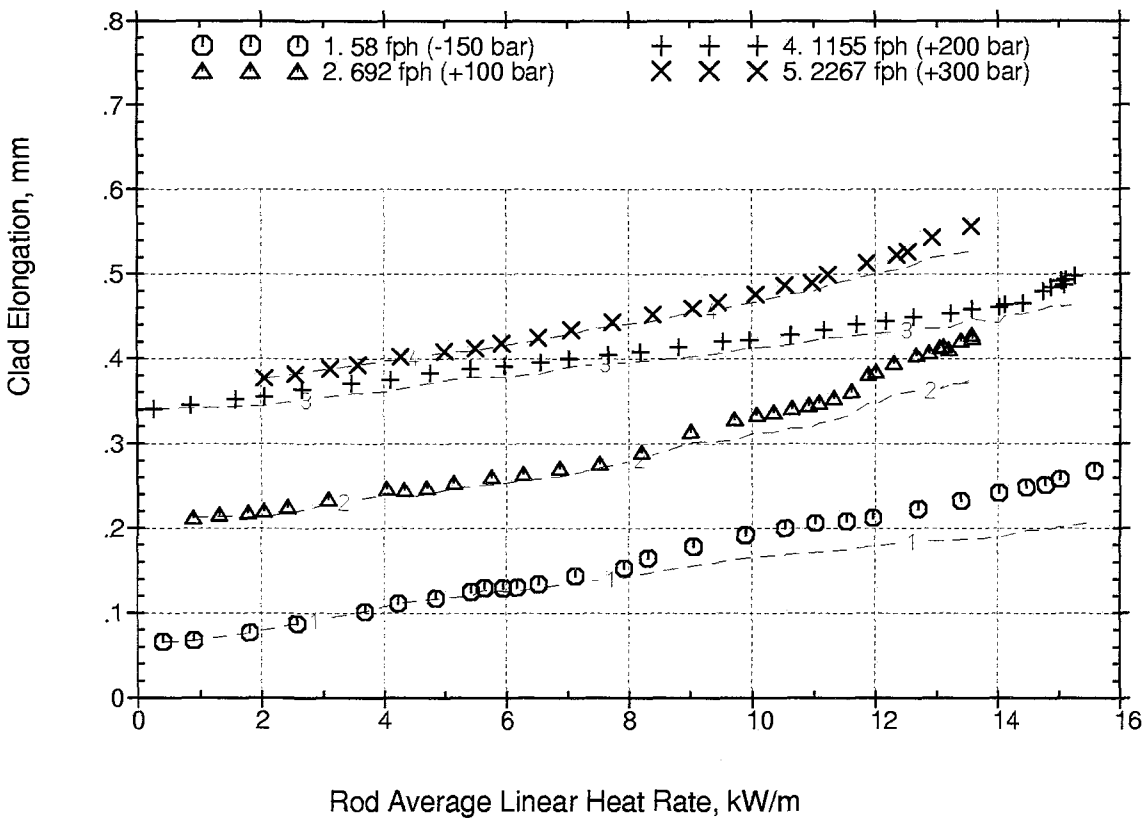

FIG. 5. Clad elongation versus average heat rate for different power ramps. The dashed lines show the estimated free thermal expansion of the cladding.

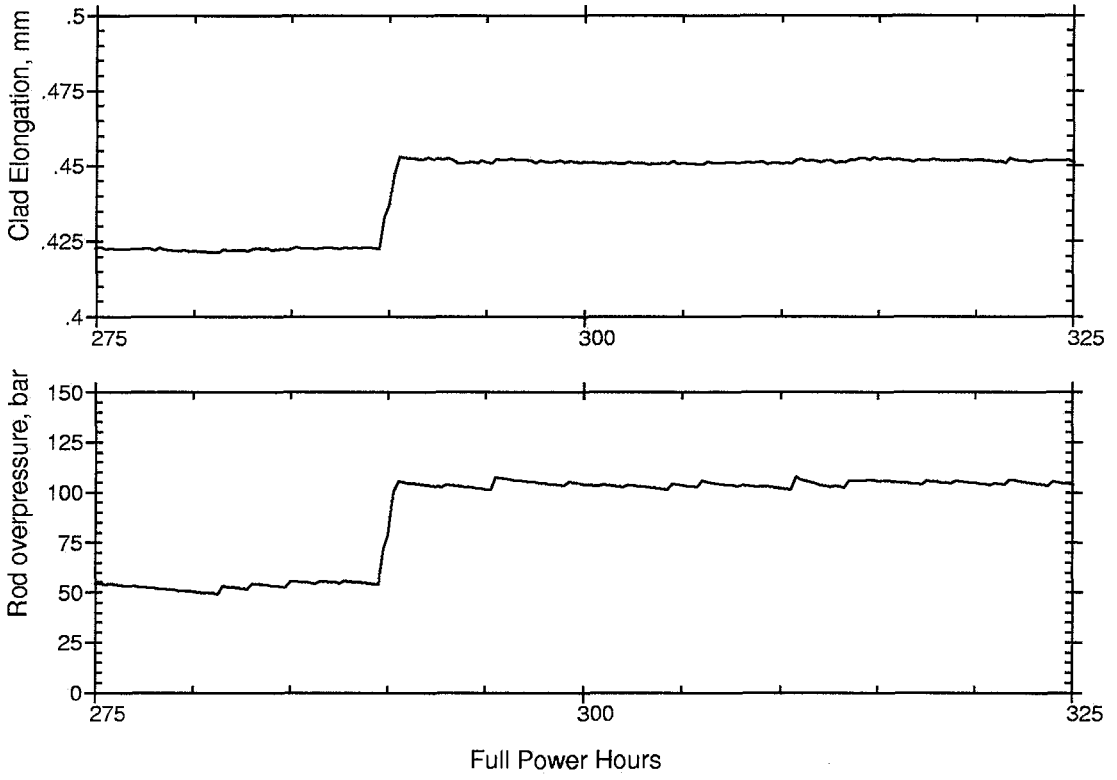

FIG. 6. Close-up of clad elongation response to pressure increase.

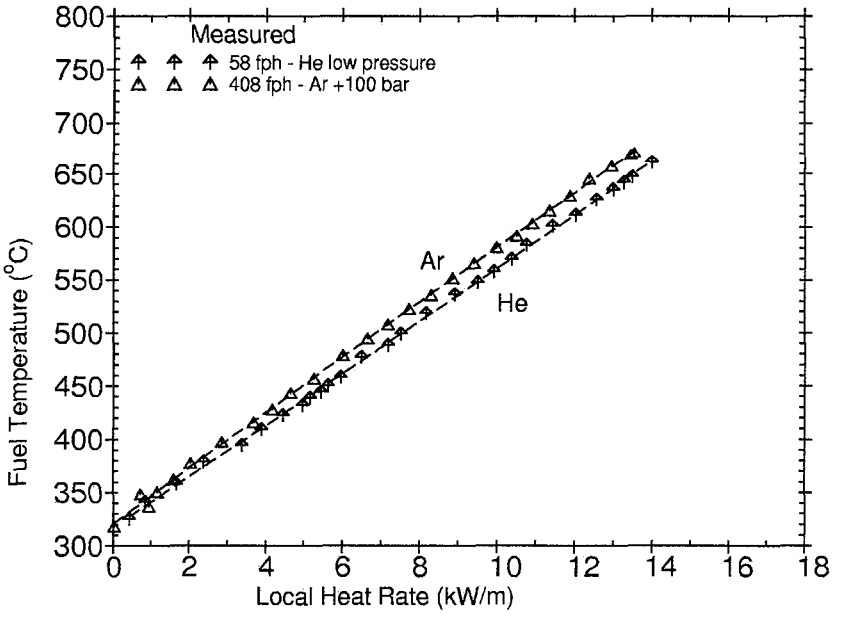

FIG. 7. Power ramps before and after first pressurisation with Ar. Dashed lines are least squares fit to the data. At 12 kW/m the temperature increase after pressurisation is 20 °C.

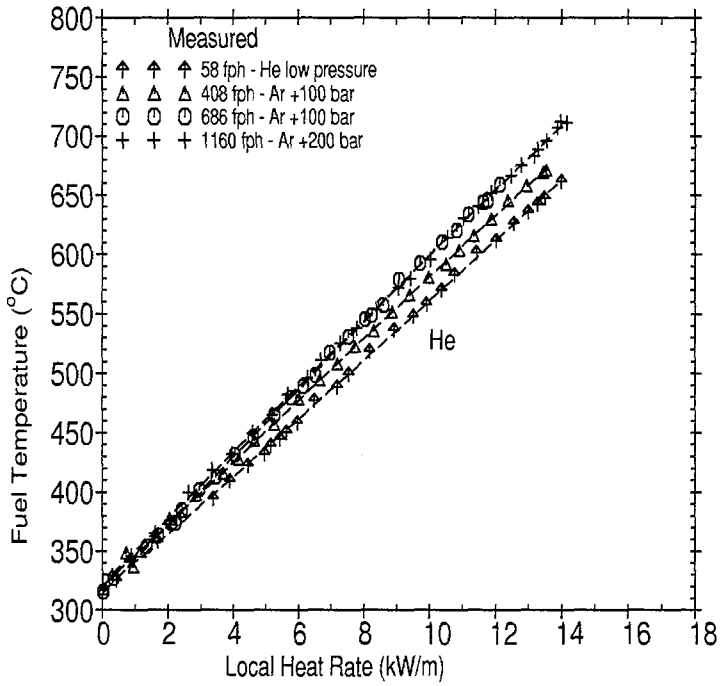

FIG. 8. The power ramps shown in figure 7 and two additional Argon ramps at pressures +100 and +200 bar. Dashed lines are least squares fit to the data.

with burnup B in MWd/kgUO_2, temperature T in °C and δ = min (T,1650). The local burnup is used in the calculations. The correlation above is plotted in Fig. 10 for different burnups. The outer oxide layer of the clad was assessed to be 60 μm (see table) and this value has been used in the calculations.

4.2. Assessment of fuel-clad gap

Several hydraulic diameter measurements were performed in this rod at various power levels. These measurements, summarized in Fig. 11, indicate that a cold diametral gap of 30 μm would be a reasonable value for the start of the test and this was chosen for the calculations. For this cold gap, the calculations estimate gap closure at powers between 12 and 15 kW/m, which is consistent with the observed clad elongation data.

4.3. Temperature calculation

Fig. 12 shows the He-ramp shown in Fig. 7 together with calculations using the assumptions stated above. A reasonably good fit to the data is obtained. Included in the figure are also temperature calculations for fresh fuel (leaving the other parameters unchanged) illustrating the influence of conductivity degradation. This amounts to ca. 100°C at 12 kW/m.

Indicated in Fig. 12 is also the first argon ramp, shown in Fig. 7. When 100% Ar is assumed as fill gas, the temperatures are somewhat overestimated. A possible explanation for this could be that there is still some helium trapped in the fuel rod at the time of the first argon ramp. After the pre-pressurisation and the first ramp (with He at 58 fph), some helium gas could have been trapped inside the rod when the gap is closed at power. Most of this helium was probably released when the internal Ar overpressurisation later on was increased from 50 to 100 bar, but the rest possibly only at the scram and following up-ramp at 408 fph. A calculation for this ramp using a gas mixture of 25% He/75% Ar shown in the figure gives a better fit to the measured data.

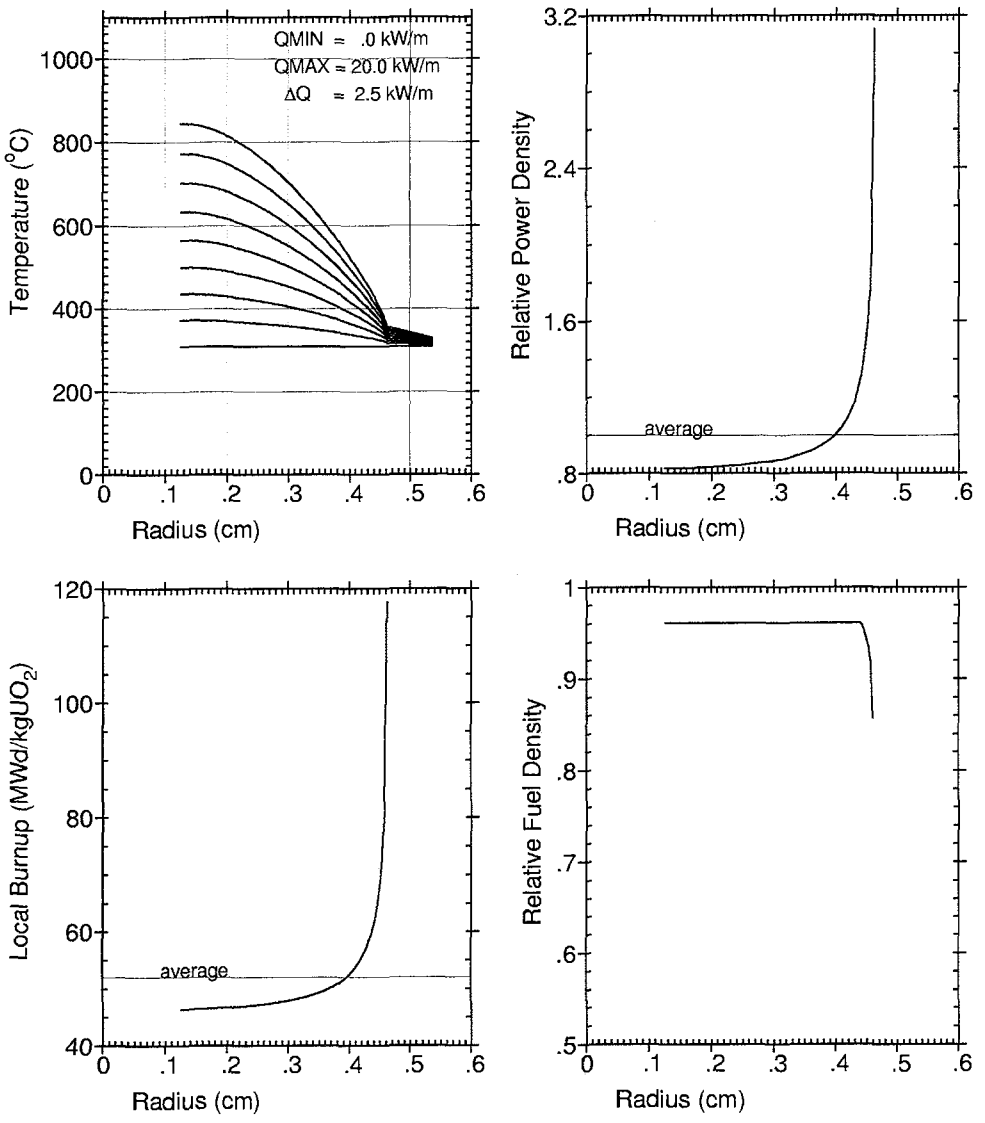

FIG. 9. Radial power and burnup distribution.

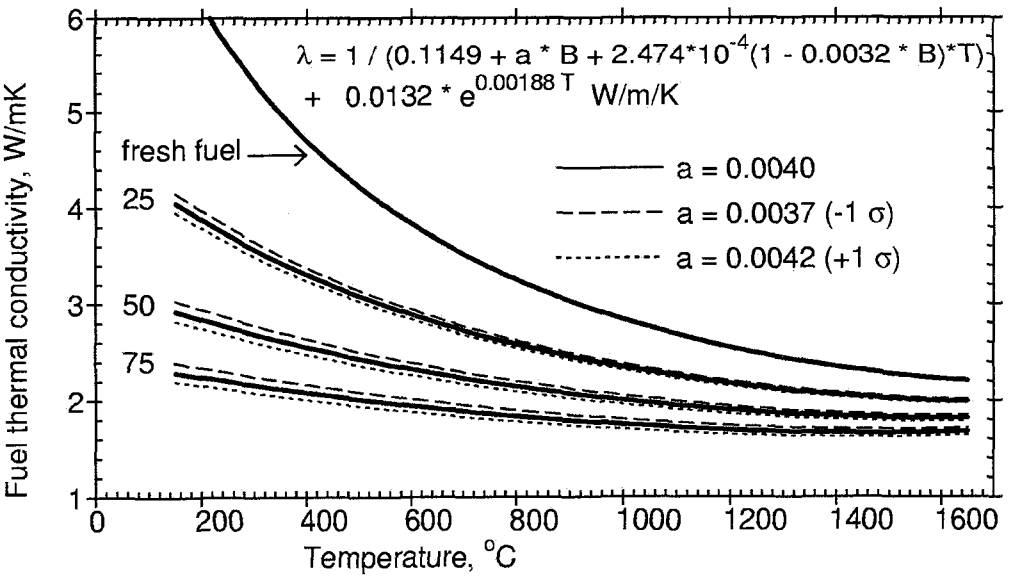

FIG. 10. Fuel thermal conductivity correlation.

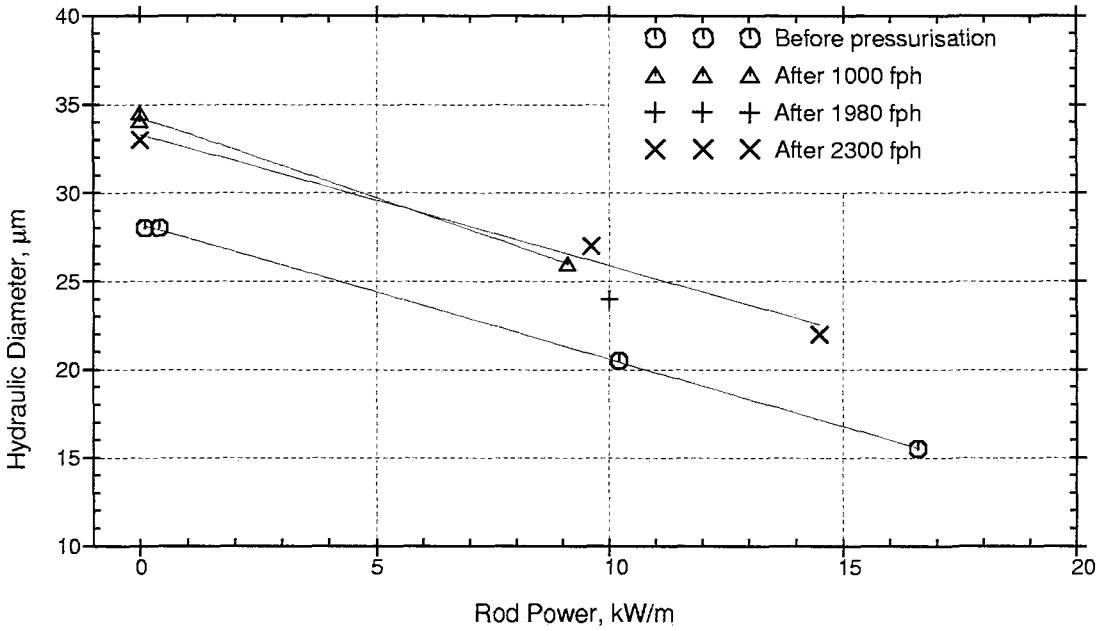

FIG. 11. Hydraulic diameter measurements.

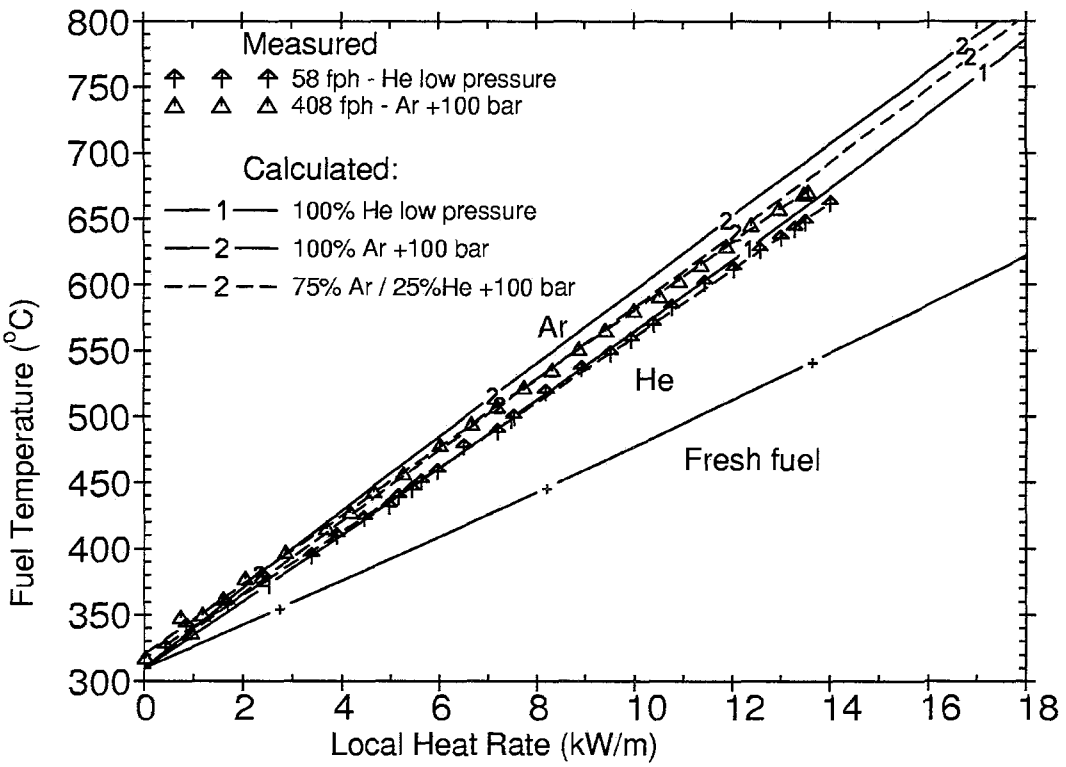

FIG. 12. The ramps in Fig. 7 together with calculations. For the Argon ramp, a gas composition of 25% He and 75% Ar gives a reasonable fit to the data.

Fig. 13 shows calculations for all ramps. Apart from the above mentioned first argon ramp, there is good agreement between measured and calculated temperatures. Note that in all calculations a cold gap of 30 μm is assumed. The elastic deformations observed in the clad elongation measurements correspond to a 2 μm diametral elastic deformation per 50 bar pressure step (see Appendix I), i.e. an 8 μm gap increase for the +200 bar ramp compared with the He ramp at low pressure. Adjusting the gap in the calculations according to the above, gives about 10°C higher temperatures at 12 kW/m. The fact that this temperature increase is not seen in the measured data, may be an indication that fuel bonding is occurring in the rod.

4.4 Scram data

Several reactor scrams were recorded and time constants calculated during the period of irradiation for this rod and are shown in Fig. 14. The calculated fuel time constant is related to the overall conductance in the rod during the transient. Given the small difference in rod burnup between the scrams, progressing conductivity degradation will have only a small influence on the fuel conductivity. It can thus be assumed, that the main changes in fuel time constant are due to differences in gap conductance. Fig. 15 shows the calculated time constant plotted versus argon pressure. While the time constants for different levels of Ar pressure are basically the same, the time constant for the scram performed during He pressurisation is considerably lower.

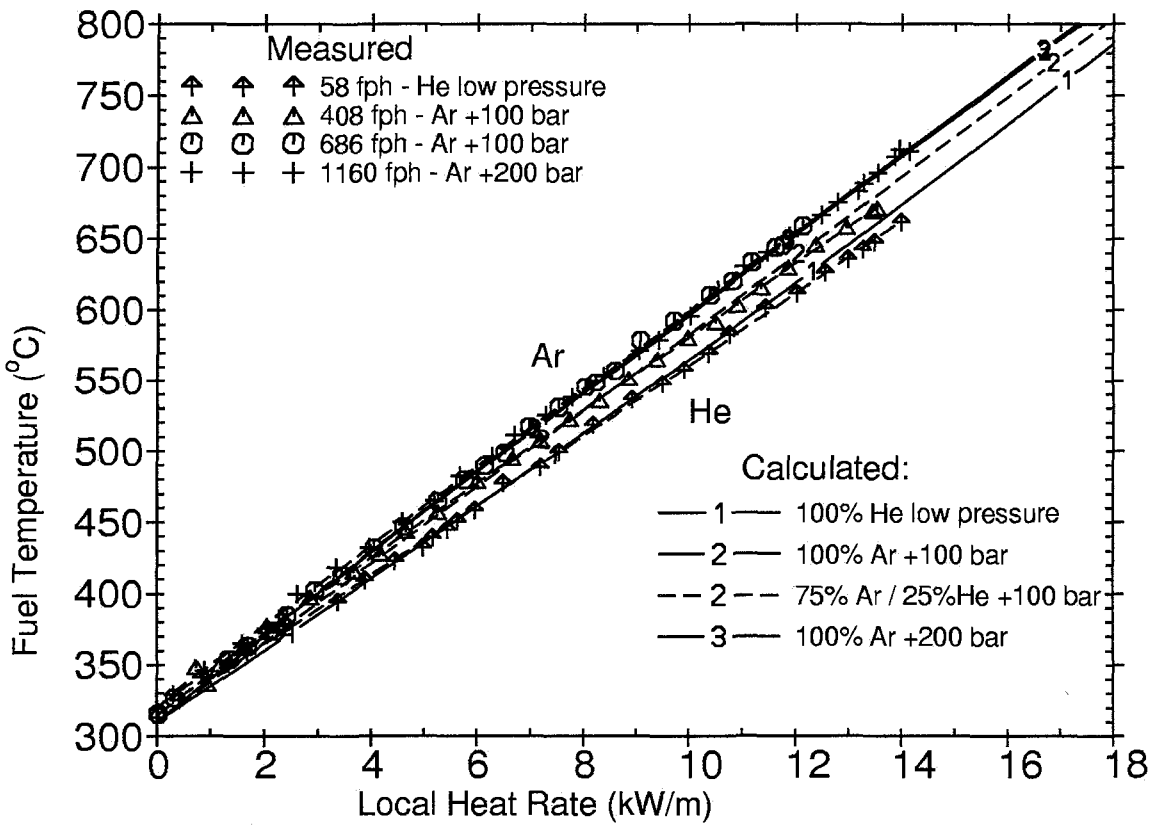

FIG. 13. All ramps in figure 8 together with calculations.

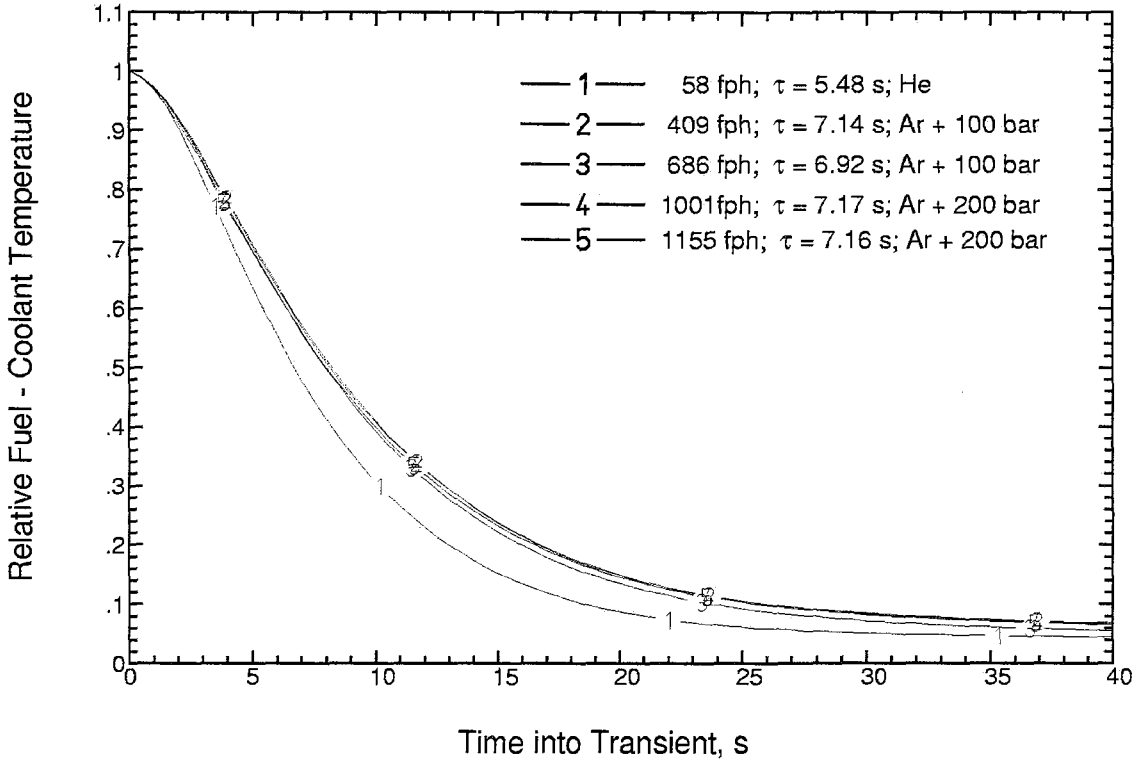

FIG. 14. Fuel temperature response to scram with calculated fuel time constants. The temperatures are normalised to initial differential fuel-coolant temperature.

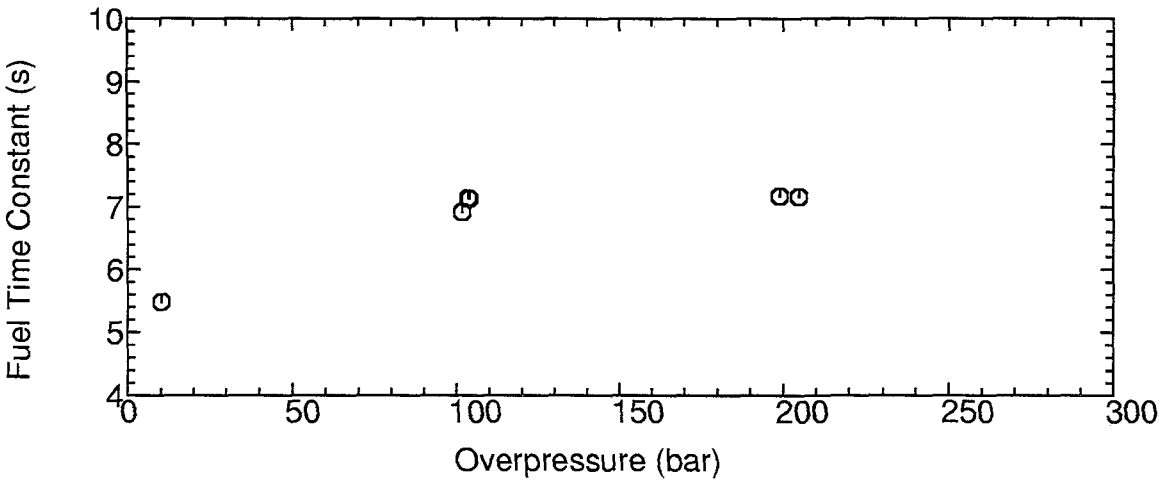

FIG. 15. Calculated fuel time constants.versus argon content.

5. SUMMARY

- Clad elongation data show that there is contact between pellet and cladding throughout the irradiation. The observed permanent clad elongation increase is in the range of fuel swelling.
- Temperatures can be modelled using as-measured gap and gas composition.
- Fuel thermal degradation is the main contributor to temperature increase compared with fresh fuel.
- Change of fuel temperature due to replacing He with Ar as fillgas (equivalent to a Xe/He gas mixture of 70%/30%) are relatively small because of the narrow or closed gap prevailing in high burnup fuel.

REFERENCES

[1] OHIRA, K., ITAGAKI, N.: "Thermal conductivity measurements of high burnup UO_2 pellets and a benchmark calculation of fuel centre temperature", Light Water Reactor Fuel Performance (Proc. Int. Topical Mtg Portland, Oregon, March 1997), ANS (!997) 541.

[2] WIESENACK, W.: "Assessment of UO_2 conductivity degradation based on in-pile temperature data," Light Water Reactor Fuel Performance (Proc. Int. Topical Mtg Portland, Oregon, March 1997), ANS (!997) 507.

[3] TVERBERG, T.: "Studies of PCMI from Cladding Elongation Measurements Performed in the HBWR", Fuel Chemistry and Pellet-Clad Interaction Related to High Burnup Fuel Proc. IAEA TCM Nyköping, Sweden September 1998), in press.

[4] LASSMANN, K., O'CARROLL, C., VAN DE LAAR, J., WALKER, J.T.:" The radial distribution of plutonium in high burnup UO_2 fuels", J. of Nucl. Mat. **208** (1994) 31.

[5] WIESENACK, W., TVERBERG, T.: "Thermal performance of high burnup fuel - in-pile temperature data and analysis", Light Water Reactor Fuel Performance, (Proc. Int. Topical Mtg Park City, Utah, April 2000), ANS (2000) 626.

[6] HAGRMAN, D. L., REYMANN, G. A. (eds.): "MATPRO version 11-A Handbook of Materials Properties for Use in the Analysis of Light Water Reactor Fuel Rod Behaviour", TREE-NUREG-1280, February 1979

Appendix I

CALCULATION OF ELASTIC STRAIN

With the following abbreviations and nomenclature:

$$A = \frac{a^2 p_i - b^2 p_0}{b^2 - a^2} \qquad and \qquad B = \frac{(p_i - p_0) \cdot a^2 b^2}{r^2 (b^2 - a^2)}$$

where:

a = initial tube inner radius,
b = initial tube outer radius,
p_i = internal pressure [MPa],
p_o = external pressure [MPa],

The radial, circumferential (hoop) and axial stresses for a thick-walled tube are:

$$\sigma_r = A - B \qquad \sigma_c = A + B \qquad \sigma_a = A$$

For a tube under an applied stress, the elastic hoop strain, $\varepsilon_{c(elastic)}$, and the elastic axial strain, $\varepsilon_{a(elastic)}$, are given by:

$$\varepsilon_{c(elastic)} = \frac{1}{E}[\sigma_c - \mu(\sigma_r + \sigma_a)] \qquad and \qquad \varepsilon_{a(elastic)} = \frac{1}{E}\left[\frac{\sigma_c}{2} - 2\mu\sigma_a\right]$$

where:

E = Young's modulus [MPa]
μ = Poisson's ratio

The radial displacement of the cladding inner wall and the cladding length change are:

$$(\Delta D) = D \cdot \varepsilon_{c(elastic)} \qquad and \qquad (\Delta L)_{elastic} = L \cdot \varepsilon_{a(elastic)}$$

where L is the cladding length.

In order to simplify these equations, one can assume

$$a \cong b \cong d \qquad and \qquad b^2 - a^2 = 2 \cdot d \cdot t$$

where d is the average diameter of the cladding and t its thickness, and obtain:

$$\frac{(\Delta D)_{elastic}}{D} = \frac{A}{E} \cdot (2 - \mu) \quad and \quad \frac{(\Delta L)_{elastic}}{L} = \frac{A}{E} \cdot (1 - 2\mu)$$

For a clad temperature of 360°C, $\mu \sim 0.25$ [6]. Thus we obtain the following relation:

$$\frac{(\Delta D)_{elastic}}{D} = 3.5 \cdot \frac{(\Delta L)_{elastic}}{L}$$

Assuming a clad length subjected to overpressure of 450 mm and a cladding inner diameter of 9.29 mm, we obtain a 2μm deformation of the inner clad wall per 50 bar pressure step.